Acta Pharmaceutica Sinica B 2025;15(1):224–238

Chinese Pharmaceutical Association
Institute of Materia Medica, Chinese Academy of Medical Sciences

Acta Pharmaceutica Sinica B

www.elsevier.com/locate/apsb
www.sciencedirect.com

ORIGINAL ARTICLE

Free fatty acid receptor-4 regulates T-cell-mediated allogeneic reaction through activating an aryl hydrocarbon receptor pathway

Maxwell Duah[a,b,†], Fei Zheng[a,b,†], Jingyi Shen[a,b,†], Yan Xu[a,b,†], Shuo Cao[a,b], Zhiling Yan[a,b], Qiu Lan[a,b], Ying Wang[a,b], Kailin Xu[a,b,*], Bin Pan[a,b,*]

[a]*Department of Hematology, the Affiliated Hospital of Xuzhou Medical University, Xuzhou Medical University, Xuzhou 221002, China*
[b]*Blood Diseases Institute, Xuzhou Medical University, Xuzhou 221002, China*

Received 12 May 2024; received in revised form 26 July 2024; accepted 27 September 2024

KEY WORDS

Free fatty acid receptor-4;
CpdA;
T-cell;
Graft-*versus*-host disease;
Allogeneic reaction;
Aryl hydrocarbon receptor;
Interleukin-22;
Obesity

Abstract Targeting T-cell is a strategy to control allogeneic response disorders, such as acute graft-versus-host disease (GVHD) which is an important cause of therapy-failure after allogeneic hematopoietic cell transplants. Free fatty acid receptor-4 (FFAR4) is a regulator of obesity but its role in T-cell and allogeneic reactions is unknown. Here, we found knockout of *Ffar4* in donor T-cells in a mouse allograft model increased acute GVHD whereas the natural FFAR4 ligands and the synthetic FFAR4 agonists decreased it. FFAR4 agonist-mediated anti-acute GVHD effects depended on FFAR4-expression in donor T-cells. The FFAR4 agonist CpdA suppressed donor T-cell-mediated alloreaction by activating an aryl hydrocarbon receptor (AhR) pathway. CpdA recruited β-Arrestin2 to FFAR4 which facilitated nuclear translocation of AhR and upregulation of IL-22. The CpdA-mediated anti-acute GVHD effect was absent in mice receiving *Ahr*-knockout or *Il22*-knockout T-cells. Recipient-expressing *Ffar4* was also important for the anti-acute GVHD effect of CpdA which inhibited activation of antigen presenting cells. Importantly, CpdA decreased acute GVHD in obese mice, an effect also depended on *Ffar4*-expression in donor T-cells and recipients. Our study shows the immunoregulatory effect of FFAR4 in T-cell, and targeting FFAR4 might be a relative option for controlling allogeneic reactions in obese patients.

*Corresponding authors.
E-mail addresses: panbinsam@163.com (Bin Pan), xukl@xzhmu.edu.cn (Kailin Xu).
[†]These authors made equal contributions to this work.
Peer review under the responsibility of Chinese Pharmaceutical Association and Institute of Materia Medica, Chinese Academy of Medical Sciences.

https://doi.org/10.1016/j.apsb.2024.12.011

1. Introduction

T-cells are crucial mediators of allogeneic reactions. Acute graft-*versus*-host disease (GVHD) is an important cause of failure after allogeneic hematopoietic cell transplants[1]. Therapies for acute GVHD are often ineffective[2]. Acute GVHD results from the alloreaction between donor T-cells and recipient antigen presenting cells (APCs)[1]. Strategies that simultaneously target T-cells and APCs might be ideal options to prevent or control acute GVHD.

Free fatty acid receptor-4 (FFAR4), also termed G protein-coupled receptor 120 (GPR120), exerts an anti-inflammatory effect in macrophages[3]. FFAR4 is the receptor for long-chain fatty acids such as polyunsaturated fatty acids (PUFAs) including docosahexaenoic acid (DHA), eicosapentaenoic acid, linoleic acid, etc.[4]. High PUFAs diet characterizes Eastern Mediterranean region and Japanese populations who were reported to have lower incidences of acute GVHD[5,6]. One un-replicated small study reported administration of eicosapentaenoic acid reduced levels of pro-inflammatory cytokines and increased survival of allotransplant recipients[7]. These data suggest PUFAs might negatively regulate pathogenesis of acute GVHD. In addition, FFAR4 agonist alleviated macrophage-induced inflammation in obesity[8,9]. Transplant recipients often have co-morbidities such as obesity which is associated with worse survival[10,11]. Allotransplanted mice with diet-induced obesity (DIO) have increased pro-inflammatory cytokine production, decreased survival and increased acute GVHD compared with regular recipients[12]. Humans and mice with obesity-related diabetes also have pro-inflammatory features[13,14]. These findings indicated targeting FFAR4 might be possible to control acute GVHD, especially in obese recipients.

Effects of FFAR4 on allogeneic T-cell functions are unknown. We found the natural ligands and synthetic agonists of FFAR4 decreased acute GVHD in mice receiving an allotransplant, whereas knockout of *Ffar4* in donor T-cells increased acute GVHD. FFAR4 agonist-mediated anti-acute GVHD effects depended on *Ffar4*-expression in donor T-cells. The FFAR4 agonist suppressed donor T-cell-mediated alloreaction by activating an aryl hydrocarbon receptor (AhR) pathway. Importantly, FFAR4 agonism decreased the severity of acute GVHD in obese mice, an effect also depended on FFAR4.

2. Materials and methods

2.1. Mice

Wild type BALB/c and C57BL/6 (B6) mice (6−8 weeks) were purchased from Charles River Laboratories (Vital River, Beijing, China). B6/JGpt-*Ffar4*^{em1Cd}/Gpt (*Ffar4*KO) mice and B6/JGpt-*Lep*^{em1Cd25}/Gpt (*Lep*^{ob}) obese mice (with obesity-related diabetes) were obtained from Model Animal Research Center of Nanjing University (Nanjing, China). *Il22*-knockout (*Il22*KO) mice (generated by Transcription Activator-Like Effector Nuclease Technology), B6-*Lck-cre;Ahr*$^{fl/fl}$ mice and B6-*Cd11c-cre;Ahr*$^{fl/fl}$ mice (*Ahr*-knockout, *Ahr*KO) were obtained from Cyagen (Suzhou, China). DIO mice were obtained by feeding mice with high-fat diet (40% fat) from 4- to 12-week old. Mice were bred in a specific-pathogen-free room. Procedures regarding animal care and experiments were approved by Medical Ethics Committee of Xuzhou Medical University (Xuzhou, China).

2.2. Cells

T-cells were purified from B6 mice spleen cells using the EasySep Mouse T Cell Isolation Kit (19851, STEMCELL Technologies, Shanghai, China) and cultured in RPMI-1640 medium (Sigma−Aldrich, Shanghai, China) with Dynabeads Mouse T-Activator CD3/CD28 (11452D, ThermoFisher Scientific, Waltham, MA, USA) for 48 h. Bone marrow-derived dendritic cells (BMDCs) were obtained from BALB/c mice as described and cultured for 7 days in RPMI-1640 medium supplied with 10% FBS and 20 ng/mL recombinant murine GM-CSF[15]. On Day 6, lipopolysaccharide (LPS) was added (working concentration: 100 ng/mL). On Day 7, LPS-primed BMDCs were co-cultured with T-cells at a ratio of BMDC:T-cell = 1:5 in RPMI-1640 medium supplied with 10% FBS. Peritoneal macrophages were obtained from BALB/c mice by flushing the abdominal cavity with PBS buffer. Macrophages were cultured in Dulbecco's modified Eagle's medium (DMEM) medium (ThermoFisher Scientific). Mixed lymphocyte reaction (MLR) was performed by co-culturing lymphocytes of BALB/c and B6 mice. B6 lymphocytes were used as reactive cells, and irradiated (3.0 Gy) BALB/c lymphocytes were stimulating cells. Lymphocytes were isolated from spleens using a lymphocyte separation buffer (7211012, DAKEWE, Shenzhen, China). Jurkat cells (ATCC TIB-152), a human T-cell line, were cultured in RPMI-1640 medium (Sigma−Aldrich). The cells were negative in mycoplasma detection.

2.3. Reagents

CpdA (C5824), GW9508 (A1709) and TUG891 (B5651) were from ApexBio (Houston, TX, USA). Recombinant murine GM-CSF (AF-315-03) and IL-22 (AF-210-22) were from PeproTech (Rocky Hill, NJ, USA). LPS (Sigma−Aldrich, 055:B5, L2880) was from Merck (Shanghai, China). DHA (HY-B2167), myristic acid (HY-N2041), oleic acid (HY-N1446), linoleic acid (HY-N0729), FFAR4 antagonist AH-7614 (HY-19996), PKA inhibitor H-89 dihydrochloride (HY-15979A), PKC inhibitor chelerythrine chloride (HY-12048), AhR agonist FICZ (HY-12451), phorbol 12-myristate 13-acetate (PMA, HY-18739), ionomycin (HY-13434) and brefeldin A (HY-16592) were from MedChemExpress (Monmouth Junction, NJ, USA). The chemical structures of compounds are in Supporting Information Fig. S1.

2.4. Transplants

In the B6 → BALB/c model, BALB/c recipients received 7.5 Gy total body radiation from a ^{137}Cs source followed by an infusion of $5 \times 10E^{+6}$ T-cell-depleted bone marrow (TCD-BM) cells and $2.5 \times 10E^{+6}$ spleen T-cells from wild type or genetically modified

B6 mice. In the BALB/c → B6 model, wild type or genetically modified B6 recipient mice received 9.0 Gy total body radiation followed by an infusion of $5 \times 10E^{+6}$ TCD-BM cells and $5 \times 10E^{+6}$ spleen T-cells from BALB/c donors. Recipient mice were intra-peritoneally injected with vehicle or different doses FFAR4 agonists/ligands thrice weekly for 3 w post-transplant[8,16,17]. Recipient mice transplanted with donor TCD-BM cells alone were used as GVHD-negative controls. The irradiated recipient mice were randomly allocated into each group. Survival of recipients were continuously observed.

2.5. Assessment of acute GVHD

Signs of acute GVHD were assessed using acute GVHD scores as described[18]. The left liver lobe and descending colon were collected and acute GVHD features of these tissues were assessed by hematoxylin and eosin (H&E) staining and histological analyses. Liver GVHD was assessed for infiltration of inflammatory cells into portal tracts. Colon GVHD was assessed for apoptotic bodies in crypts and inflammatory cells in lamina propria. Histological scores were determined by two blinded pathologists[19].

2.6. Multiparameter flow cytometry

T-cells were stained with PerCP-Cy5.5-anti-CD3 (100326, BioLegend, San Diego, CA, USA), BV421-anti-CD4 (100544, BioLegend), PE-Cy7-anti-CD8 (100714, BioLegend) and AF647-anti-FFAR4 (NBP1-00858AF647, Novus Biologicals, Littleton, CO, USA) to detect FFAR4. Dendritic cells and macrophages were stained with AF647-anti-FFAR4 and FITC-anti-CD11c (117306, BioLegend) or PE-anti-MHC-II (107608, BioLegend) to detect FFAR4. AF647-Rabbit IgG (NBP2-24891AF647, Novus Biologicals) was used as isotype control. Spleen cells were incubated with PMA, ionomycin and Brefeldin A for 4 h at 37 °C followed by processing with Fixation/Permeabilization Solution (554715, BD Biosciences, San Jose, CA, USA) to detect effector T-cells. Cells were stained with PerCP-Cy5.5-anti-CD3, FITC-anti-IFNγ (554411, BD Biosciences) and PE-anti-IL-22 (516404, BioLegend). Cells were acquired on a LSRFortessa flow cytometer (BD Biosciences), and analyzed by FlowJo 7.6 software.

2.7. Western blotting

Whole cell proteins were extracted using Cell Lysis Buffer (9803, Cell Signaling Technology, Danvers, MA, USA). The NE-PER kit (78833, ThermoFisher Scientific) was used to separate cytoplastic and nuclear proteins. The following antibodies were used: FFAR4 (NBP1-00858) was from Novus Biologicals. STAT1 (9172), p-STAT1 (9167), STAT3 (4904), p-STAT3 (9145), STAT5 (94205), p-STAT5 (9359), p65 (8242), p-p65 (3033), ERK (9102), p-ERK (9101), p38 (9212), p-p38 (9211), GRK2 (74761) and GRK6 (5878) were from Cell Signaling Technology. JNK (24164-1-AP), p-JNK (80024-1-RR), AhR (67785-1-Ig), ARNT (14105-1-AP), β-Arrestin2 (10171-1-AP), β-Arrestin1 (67580-1-Ig), GRK5 (17032-1-AP), TAK1 (12330-2-AP), p-TAK1 (28958-1-AP), HSP90AB1 (80301-1-RR), Histone-H3 (17168-1-AP) and β-actin (20536-1-AP) were from Proteintech (Carlsbad, CA, USA).

2.8. Immunoprecipitation

Cell proteins were pulled down with anti-β-Arrestin2 (10171-1-AP, Proteintech) and Protein A Magnetic Bead (LSKMAGA02, Merck) to detect β-Arrestin2 binding proteins. The precipitate was analyzed by Western blotting with antibodies including AhR (67785-1-Ig, Proteintech), ARNT (14105-1-AP, Proteintech), FFAR4 (BF8192, Affinity Biosciences), HSP90AB1 (80301-1-RR, Proteintech) and β-Arrestin1/2 (sc-53781, Santa Cruz Biotechnology, Dallas, TX, USA). A pull-down assay was done with anti-AhR (28727-1-AP, Proteintech) and anti-ARNT (14105-1-AP, Proteintech) to detect binding of AhR and ARNT. Protein A Magnetic Bead-precipitated proteins were detected with anti-ARNT (14105-1-AP, Proteintech), anti-AhR (67785-1-Ig, Proteintech), β-Arrestin2 (10171-1-AP, Proteintech) and HSP90AB1 (80301-1-RR, Proteintech). Rabbit IgG (30000-0-AP, Proteintech) was a negative control for pull-down assay.

2.9. Immunofluorescence

Immunofluorescence was performed with T-cells and BMDCs. Briefly, cells were incubated with anti-AhR (28727-1-AP, Proteintech) for 4 h at room temperature. CoraLite594-conjugated goat anti-rabbit IgG (SA00013-4, Proteintech) was used as the second antibody for visualization. T-cells and BMDCs were simultaneously stained with CoraLite Plus 488 anti-mouse CD3ε (CL488-65061, Proteintech) and CoraLite Plus 488 anti-mouse CD11c (CL488-65130, Proteintech), respectively. DAPI was used to stain nuclei. Photos were acquired on a Zeiss 880 confocal microscope (Oberkochen, Germany).

2.10. Quantitative PCR

Total RNA isolation and cDNA synthesis were performed as described[15]. Quantitative PCR (qPCR) was done using LightCycler 480 SYBR Green I Master kit (4887352001, Roche, Mannheim, Germany). Primers are indicated in Supporting Information Table S1. GAPDH was used as a normalization gene. Relative mRNA levels were $-\Delta\Delta C_T$ values.

2.11. RNA-seq

Spleen T-cells were stimulated with CD3/CD28 Dynabeads for 48 h followed by incubation with vehicle or 10 μmol/L CpdA for 24 h, and total RNA was extracted. NEBNext Ultra RNA Library Prep Kit for Illumina (E7530, NEB, Ipswich, MA, USA) was used to generate sequencing libraries. RNA-seq was performed on a NovaSeq 6000 platform. Bioinformatics analyses were performed by Genechem (Shanghai, China). RNA-seq data are available at NCBI Sequence Read Archive (PRJNA918719).

2.12. Detection of free fatty acids

Plasma samples were analyzed at Sci-Tech Innovation (Qingdao, China) for long-chain free fatty acids. Fatty acid standards were purchased from Merck. Detection was done on a Trace1310 ISQ Gas chromatography−mass spectrometry (Thermo Fisher Scientific).

2.13. Detection of tryptophan metabolites

Fecal samples were collected from mice. A 50 mg aliquot of each sample was homogenized in 0.5 mL extraction buffer (methanol:acetonitrile:H_2O = 2:2:1, *v*/*v*/*v*). The supernatant was dried by nitrogen stream evaporation, re-dissolved in

0.1% (*v*/*v*) formic acid water solution and the supernatant was analyzed by UHPLC−MS/MS using the EXIONLC System and SCIEX 6500 QTRAP + triple quadrupole mass spectrometer (SCIEX, Framingham, MA, USA). A list of tryptophan metabolites is displayed in Supporting Information Table S2. Standards were from BIOTREE (Shanghai, China). The concentrations of tryptophan metabolites were calculated from the standard curves.

2.14. Transfection

Transfection of mouse T-cells with siRNAs was by electroporation with the P3 Primary Cell 4D-Nucleofector X Kit L (V4XP-3024, Lonza, Cologne, Germany) on a Lonza 4D Nucleofector. siRNAs included:

Arrb1 siRNA-1: CCAACAAGACUGUGAAGAA,
Arrb1 siRNA-2: CUGAGAACCUGGAGGAGAA,
Arrb1 siRNA-3: CCUACAAAGUCAAGGUGAA,
Arrb2 siRNA-1: CCUACAGGGUCAAGGUGAA,
Arrb2 siRNA-2: AGGGAAGGCUUGUGGAGUA,
Arrb2 siRNA-3: ACAAAGAGCUGUACUACCA.

A scrambled siRNA was used as negative control. siRNAs were synthesized by General Biol (Hefei, China). In our preliminary experiment a mixture of three pairs of siRNAs had the highest knockdown efficacy.

2.15. Cell viability

CCK-8 reagent (CK04, DOJINDO, Tokyo, Japan) was used to assess cell viability by measuring optical density at 450 nm.

2.16. TdT-mediated dUTP nick end labeling (TUNEL)

Colon tissue slides were processed using a TUNEL kit (KGA1401, Keygen Biotech, Nanjing, China). Following visualization of apoptotic cells (brown), the slides were counterstained with hematoxylin. Apoptotic cells were counted.

2.17. Detection of cytokine concentrations

Cytometric beads array (552364, BD Biosciences) was performed on a flow cytometer for measuring concentrations of IL-6, TNFα and IFNγ. Enzyme-linked immune absorbent assay was used to measure concentration of IL-22 (900-K257, ThermoFisher Scientific).

2.18. Statistical analyses

GraphPad Prism 6.0 was used for statistical analyses. Data were displayed as individual values or mean ± standard deviation (SD). Survival data were displayed by Kaplan−Meier curves and compared using the log-rank test. Comparisons of means were done using 2-tailed unpaired Student's *t* test or one-way ANOVA test. *P*-values <0.05 were considered significant.

3. Results

3.1. FFAR4 agonism decreased murine acute GVHD

In the B6 → BALB/c allotransplant model, plasma concentrations of long-chain fatty acids showed dynamic changes between Days 10 and 30 posttransplant when recipient mice developed acute GVHD. DHA (C22.6N3) and arachidonic acid (C20.4N6) showed a 1.9-fold and a 1.4-fold increase between Days 10 and 30, while oleic acid (C18.1N9C) and α-linolenic acid (C18.3N3) showed a 0.8-fold and a 0.5-fold decrease, whereas some others did not show any changes such as myristic acid (C14.0) and linoleic acid (C18.2N6C) (Supporting Information Fig. S2). In flow cytometry analyses, FFAR4 intensity on spleen T-cells showed an increase (4.8-fold for $CD4^+$ T-cell; 5.0-fold for $CD8^+$ T-cell) on Day 10 posttransplant compared with pretransplant, while FFAR4 intensity on CD11c-positive cells showed a 4.1-fold increase. FFAR4 protein level also increased on Day 10 (Supporting Information Fig. S3). Increased FFAR4 expression was also found in T-cells from *in vitro* MLR (Fig. S3).

Recipient mice were intra-peritoneally injected with different long-chain fatty acids including DHA, myristic acid, oleic acid and linoleic acid. DHA and linoleic acid increased survival and decreased signs of acute GVHD of recipient mice. Linoleic acid showed a more significantly protective effect comparing with DHA (Supporting Information Fig. S4). The protective effect of linoleic acid was abolished by concurrent treatment with the FFAR4 antagonist AH-7614 (Fig. S4). There are several synthetic FFAR4 agonists with high affinity in activating FFAR4[20]. Recipient mice were treated by three FFAR4 agonists including CpdA, GW9508 and TUG891. The agonists increased recipient survival and decreased signs of acute GVHD (Fig. S4). Because CpdA showed a more significant anti-acute GVHD effect comparing with the other two agonists, we further explored the actions of CpdA. In the B6 → BALB/c model, CpdA increased recipient survival and decreased acute GVHD scores at the doses of 30 and 90 mg/kg (Fig. 1A). The anti-acute GVHD effect of CpdA was abolished by knockout of *Ffar4* in donor T-cells (Fig. 1B). Vehicle-treated mice showed acute GVHD histological features in colon and liver which were ameliorated by CpdA. TUNEL assay showed CpdA decreased crypt apoptotic bodies in colon tissues (Fig. 1C), and these effects also depended on *Ffar4*-expression in donor T-cells (Fig. 1D). Flow cytometry analysis showed CpdA reduced IFNγ-positive spleen T-cells in recipients receiving wild type T-cells but not in those receiving *Ffar4*KO T-cells (Fig. 1E). Without CpdA treatment, mice receiving *Ffar4*KO T-cells showed increased acute GVHD compared with those receiving wild type T-cells, which was evidenced by survival, acute GVHD score, colon histological feature and percent of IFNγ-positive spleen T-cells (Fig. 1B, D and E). In another allotransplant model, injection of the FFAR4 agonists also increased recipient survival and decreased signs of acute GVHD (Fig. 1F and Fig. S4).

3.2. FFAR4 agonism inhibited MLR and altered T-cell related inflammatory profiles in vitro

CpdA decreased cell viability of the *in vitro* MLR induced by wild type cells during the 5-day culture (Fig. 2A), and the effect was absent in MLR induced by *Ffar4*KO cells (Fig. 2B). CpdA did not inhibit cell viability of non-mixed lymphocytes (Fig. 2A−C). Flow cytometry showed CpdA decreased percent of IFNγ-positive T-cells in MLR induced by wild type cells but not in MLR induced by *Ffar4*KO cells (Fig. 2D).

Inflammatory cytokines were detected in T-cells stimulated with allogeneic BMDCs or CD3/CD28 Dynabeads. CpdA reduced mRNA levels of *Il6*, *Tnf* and *Ifng* in wild type T-cells stimulated with allogeneic BMDCs, and reduced *Ifng* mRNA level in wild

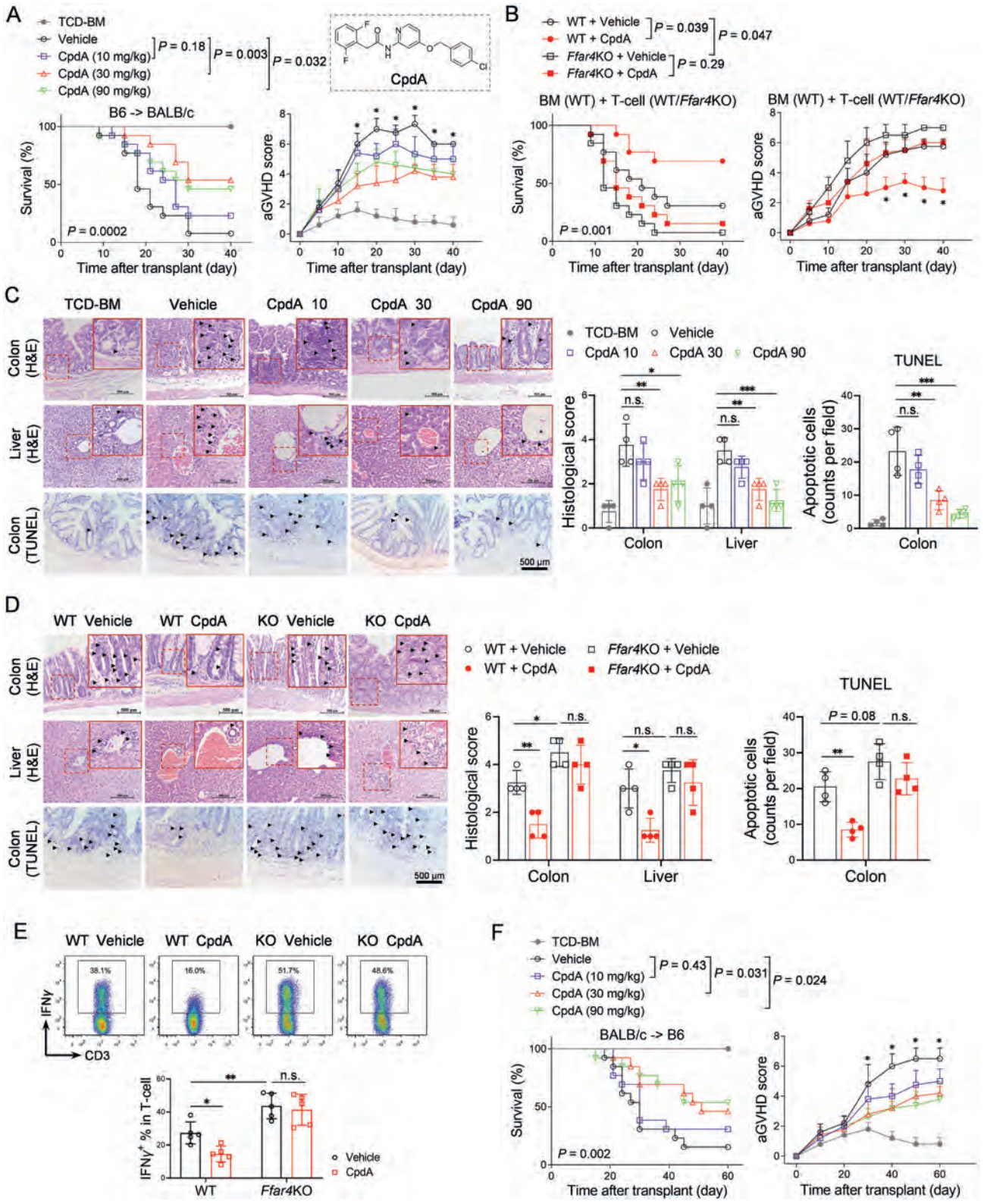

Figure 1 CpdA decreased acute GVHD (aGVHD) in murine allograft models. (A) In the B6 (donor) → BALB/c (recipient) model, recipient mice were transplanted with TCD-BM cells and spleen T-cells from donor mice. Recipient mice were injected with vehicle or different doses of CpdA thrice weekly for 3 weeks posttransplant. Survival and aGVHD score of recipient mice ($n = 18$ in each group). Recipient mice transplanted with donor TCD-BM cells alone were used as aGVHD-negative controls ($n = 8$). (B) In the B6 → BALB/c model, recipient mice were transplanted with wild type (WT) donor TCD-BM cells together with WT T-cells or *Ffar4*KO T-cells. CpdA (30 mg/kg) injection was performed as described above. Survival and aGVHD score ($n = 13$ in each group). (C, D) On Day 21, colon and liver tissues were collected from recipient mice described in Fig. 1A and B. H&E staining and histological score, TUNEL assay used for staining apoptotic cells in colon tissues ($n = 4$).

type T-cells stimulated with CD3/CD28 Dynabeads. These effects were absent in *Ffar4*KO T-cells except *Ifng* (Fig. 2E). Without CpdA treatment, *Ffar4*KO T-cells showed higher mRNA levels of *Il6* and *Ifng* comparing with wild type T-cells (Fig. 2E). We also detected the protein concentrations of these cytokines in the supernatants of cell culture, which showed similar changes as mRNA levels (Fig. 2E). The other two FFAR4 agonists also decreased mRNA and protein levels of IL-6, TNFα and IFNγ in T-cells (Supporting Information Fig. S5).

Next, we detected proteins correlated with T-cell-activation. CpdA decreased the protein levels of phosphorylated STAT1 and STAT3 in activated T-cells (Fig. 2F). CpdA did not change the levels of other proteins including phosphorylated p38, ERK, JNK, STAT5 and p65 (Supporting Information Fig. S6). In RNA-seq analyses, CpdA decreased *Ifng*-expression but increased expressions of *Il17a* and *Il2* in T-cells. Compared with wild type T-cells, *Ffar4*KO T-cells showed significantly increased expression of several pro-inflammatory cytokines such as *Il1b*, *Il12*, *Il6*, *Tnf* and *Ifng* (Fig. 2G and Supporting Information Fig. S7).

3.3. FFAR4 agonism activated aryl hydrocarbon receptor (AhR)/IL-22 in T-cells

In contrast to IFNγ-positive T-cells, CpdA increased percentage of IL-22-positive spleen T-cells in acute GVHD mice (Fig. 3A). CpdA also increased *Il22* mRNA and protein levels in cultured T-cells (Fig. 3B and Fig. S5). These effects depended on FFAR4-expression in T-cells (Fig. 3B and Supporting Information Fig. S8). In RNA-seq analyses, CpdA increased expression of *Il22*, *Il23a* and *Il23r* in T-cells (Fig. 3C). To determine if IL-22 was important for CpdA-mediated anti-acute GVHD effect, we transplanted mice with *Il22*KO T-cells. CpdA failed to increase survival or decrease acute GVHD scores in mice receiving *Il22*KO T-cells (Fig. 3D). Without CpdA treatment, *Il22*KO increased acute GVHD (Fig. 3D), which indicated a protective role of IL-22 in murine acute GVHD, and this was consistent to our previous study[21] and other study[22]. In mice transplanted with *Ffar4*KO T-cells, injection of recombinant murine IL-22 increased survival and decreased acute GVHD scores (Fig. 3E).

AhR is a key transcription factor that regulates IL-22[23]. CpdA increased expressions of *Cyp1a1* and *Cyp1b1* (Fig. 3C), which are typical downstream genes of AhR pathway[24]. Next, we explored if CpdA activated AhR. Immunofluorescence showed CpdA induced nuclear translocation of AhR in activated T-cells. Because BMDCs have abundant cytoplasm, we used CpdA to treat BMDCs and showed a clearer nuclear translocation of AhR (Fig. 3F). Western blot analysis showed CpdA-treated T-cells had more nuclear AhR protein and less cytoplasmic AhR protein compared with controls (Fig. 3G). CpdA increased *Cyp1a1* mRNA concentrations in T-cells indicating activation of AhR (Fig. 3H). We used T-cell conditional *Ahr*KO mice as donors in the B6 $\rightarrow$ BALB/c allotransplant model. Conditional knockout of *Ahr* in T-cells abolished the anti-acute GVHD effect of CpdA (Fig. 3I). These data suggest FFAR4 agonism activated the AhR pathway and the anti-acute GVHD effect depended on expressions of AhR and IL-22 in T-cells.

3.4. β-Arrestin2 regulated activation of AhR/IL-22 pathway

Next, we studied how CpdA regulated AhR/IL-22 activation in T-cells. CpdA treatment did not change mRNA levels of transcription factors which regulate expression of IL-22 (Supporting Information Fig. S9)[23]. Tryptophan metabolites are endogenous ligands of AhR[24]. Allotransplanted mice showed higher concentrations of tryptophan metabolites in the fecal samples including 5-hydroxytryptophan, kynurenine and tryptophan, comparing with mice not receiving an allotransplant. However, the FFAR4 agonists did not alter the concentrations of tryptophan metabolites in allotransplanted mice (Fig. 4A and Supporting Information Fig. S10).

FFAR4 belongs to G protein-coupled receptor family which functions through the downstream G protein-coupled receptor kinase (GRK)/β-Arrestin pathway and G-protein pathways[3]. In RNA-seq and Western blot analyses, CpdA-treatment or *Ffar4*KO decreased expression of GRK proteins (Fig. 4B and Supporting Information Fig. S11). *Ffar4*KO also decreased expression of G-protein pathways-related genes such as *Prkc* (encoding PKC) and *Prka* (PKA) (Fig. S7). CpdA might have an impact on GRK/β-Arrestin pathway and G-protein pathway. Knockdown of *Arrb2* (encoding β-Arrestin2) but not *Arrb1* (β-Arrestin1) blocked CpdA's effect in inducing expressions of *Il22* and *Cyp1a1* (Fig. 4C and Supporting Information Fig. S12). Inhibitors of PKC and PKA, at concentrations not decreasing viability of T-cells (Supporting Information Fig. S13), did not block CpdA's effect in inducing expressions of *Il22* and *Cyp1a1* (Fig. 4D). These results indicate β-Arrestin2 was involved in regulating AhR activation.

In an immunoprecipitation assay, we found CpdA induced binding of FFAR4 and β-Arrestin2 in Jurkat cells (Fig. 5A). AhR binds heat shock protein HSP90 in the cytoplasm at inactive status. When activated, AhR enters the nucleus and binds AhR nuclear translocator (ARNT)[24]. We found CpdA increased binding of AhR and ARNT (Fig. 5B). Interestingly, CpdA decreased the binding of β-Arrestin2 and AhR and the binding of β-Arrestin2 and HSP90 in the cytoplasm. ARNT did not bind β-Arrestin2 or AhR in the cytoplasm and CpdA did not induce binding of these proteins. The binding of HSP90 and AhR was detectable in the cytoplasm (Fig. 5C). The binding of AhR and ARNT was confirmed in the nucleus. We did not observe a binding of β-Arrestin2 and ARNT or a binding of β-Arrestin2 and AhR in the nucleus. HSP90 did not bind ARNT in the nucleus, but the binding of HSP90 and AhR was still detectable (Fig. 5D). The nuclear translocation of AhR induced by FICZ, an AhR agonist, was further enhanced by CpdA (Fig. 5E). The possible reason was CpdA recruited β-Arrestin2 to the cell membrane which facilitated nuclear translocation of AhR and increased binding of AhR and ARNT (Fig. 5F). Interestingly, knockdown of *Arrb2* increased

Scale bar = 500 μm. GVHD features were magnified. Black arrows indicated inflammatory cells in portal tracts of liver tissues and crypt apoptotic bodies of colon tissues. (E) On Day 21, spleen cells were isolated from recipient mice described in Fig. 1B. Flow cytometry was used to analyze IFNγ-positive spleen T-cells ($n = 5$). (F) In the BALB/c $\rightarrow$ B6 model, recipient mice were transplanted with TCD-BM cells and spleen T-cells from donor mice. CpdA injection was performed as described above. Survival and aGVHD score ($n = 8$ in TCD-BM group, $n = 18$ in other groups) were recorded. Survival was compared using log-rank test. Data were from two or three independent experiments. Data are mean $\pm$ SD, compared using one-way ANOVA test or Student's t test. $^*P < 0.05$; $^{**}P < 0.01$; $^{***}P < 0.001$; n.s., not significant.

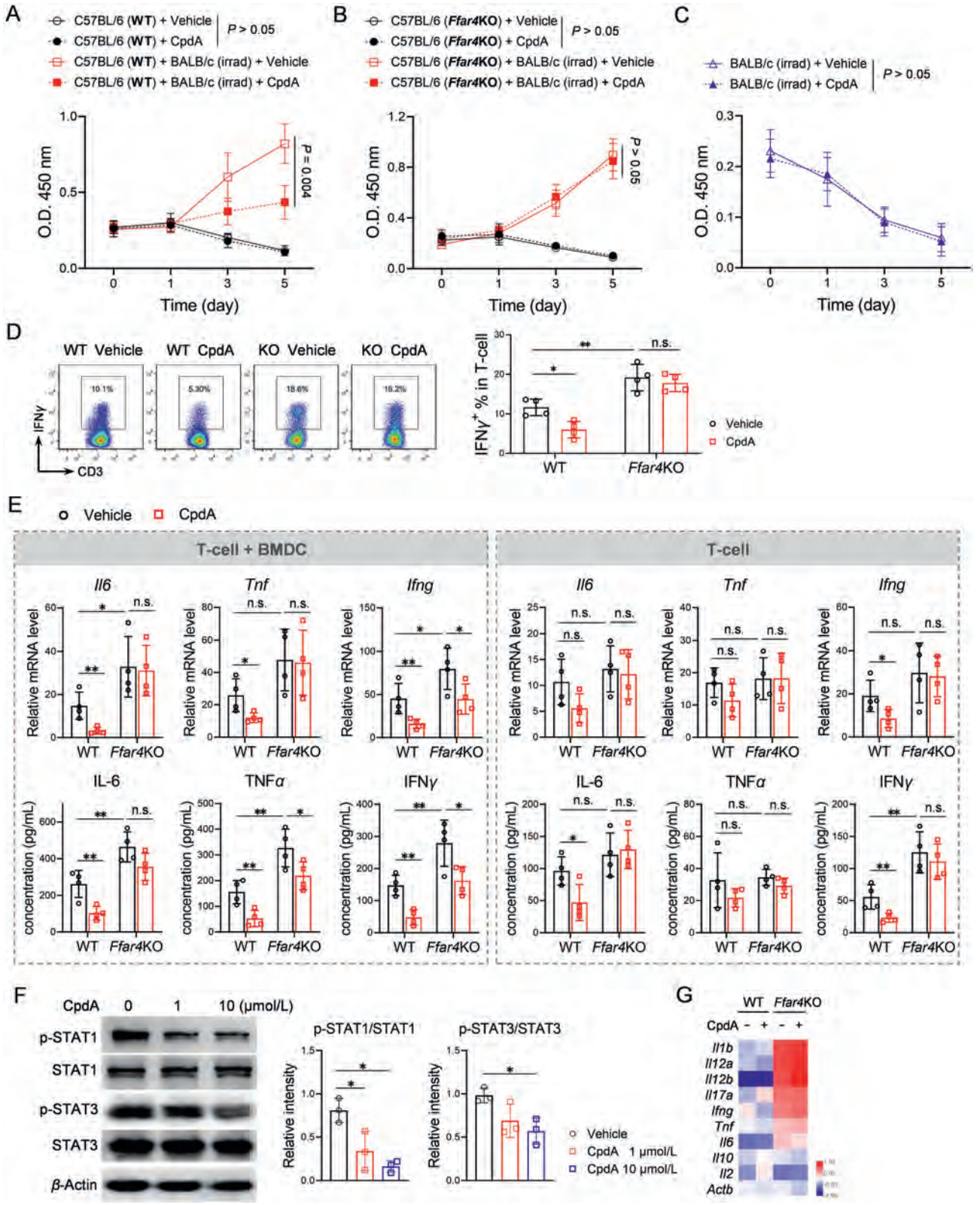

Figure 2 CpdA altered T-cell related inflammatory profiles. (A–C) Mixed lymphocyte reaction was performed by co-culturing B6 spleen lymphocytes with irradiated BALB/c spleen lymphocytes. Non-mixed lymphocytes (B6 lymphocytes or irradiated BALB/c lymphocytes cultured alone) were used as controls. Cell viability was measured by CCK-8 assay on Days 0, 1, 3 and 5 ($n = 4$). (D) Cells from mixed lymphocyte reaction were analyzed by flow cytometry for detecting IFNγ-positive T-cells ($n = 4$). (E) T-cells from WT or *Ffar4*KO B6 mice were cultured alone (stimulated by CD3/CD28 Dynabeads) or co-cultured with BALB/c BMDCs (stimulated by LPS) for 24 h in the presence of vehicle or 10 μmol/L CpdA. mRNA of cytokine was measured by qPCR ($n = 4$). mRNA levels were relative to T cells not stimulated by CD3/CD28

nuclear translocation of AhR and expressions of *Il22* and *Cyp1a1* in T-cells (Figs. 5G, H and 4C).

3.5. Recipient-expressing Ffar4 also contributed to CpdA-mediated anti-acute GVHD effect

Recipient APCs are also necessary to trigger acute GVHD[1]. In flow cytometry analyses, FFAR4 fluorescence intensity on CD11c-positive cells increased on Days 10 and 30 posttransplant compared with untreated controls (Day 0; Fig. S3). In *in vitro* cultured BMDCs and macrophages, activation of these cells with LPS increased FFAR4 expression (Fig. S3). In the BALB/c → B6 model, wild type and *Ffar4*KO B6 mice were used as recipients. CpdA increased survival and decreased acute GVHD scores of wild type recipient mice, an effect not observed in *Ffar4*KO recipients (Fig. 6A). CpdA decreased acute GVHD histological features in colon and liver from wild type recipients but not in *Ffar4*KO recipients (Fig. 6B).

Next, we used *Il22*KO mice and CD11c conditional *Ahr*KO mice as recipients. CpdA increased survival and decreased acute GVHD scores in these mice (Fig. 6C and D). In the *in vitro* cultured BMDCs, CpdA induced expression of *Cyp1a1* but not of *Il22* (Fig. 6E). These results indicated the anti-acute GVHD effect depended on recipient-expressing *Ffar4* but not recipient-derived AhR or IL-22. Others reported FFAR4 agonists regulated macrophage activation through inhibition of JNK and TAK1 pathways[9]. Using LPS-treated BMDCs, we found CpdA decreased protein levels of phosphorylated JNK, TAK1 and p65 (Fig. 6F). CpdA decreased mRNA and protein levels of IL-6 and TNFα in LPS-treated BMDCs (Fig. S5). Thus, FFAR4 agonist-mediated inhibition of APCs activation also contributed to the anti-acute GVHD effect.

3.6. CpdA alleviated acute GVHD in obese mice

We used *Lep*^{ob} obesity B6 mice as recipients in the BALB/c → B6 allotransplant model. Injection of CpdA significantly increased survival of recipient mice and decreased signs of acute GVHD (Fig. 7A). Normally bred obese mice showed extensive steatosis in liver tissues, compared with wild type mice. CpdA treatment reduced the acute GVHD features in liver and colon of recipient mice (Fig. 7B). CpdA-treated mice had decreased protein concentrations of IL-6 and TNFα but increased IL-22 concentrations in plasma samples, comparing with vehicle-treated controls (Fig. 7C). DIO BALB/c and DIO B6 mice were also used as recipients in allotransplant models. CpdA increased survival and decreased acute GVHD scores of these DIO recipient mice, and the anti-acute GVHD effects depended on donor-T-cell-expressing FFAR4 and recipient-expressing FFAR4 (Fig. 7D and E). We pooled the survival data of regular BALB/c recipients and DIO BALB/c recipients, and compared the effects of CpdA in these mice (Supporting Information Fig. S14). DIO recipients showed significantly shortened survival comparing with regular recipients. In mice transplanted with wild type donor T-cells, CpdA more effectively increased survival of DIO recipients comparing with regular recipients ($P = 0.0001$ *vs.* $P = 0.017$). In mice transplanted with *Ffar4*KO donor T-cells, CpdA failed to increase survival of regular recipients ($P = 0.29$) but still protected DIO recipients ($P = 0.013$).

4. Discussion

We show knockout of *Ffar4* in donor T-cells in a mouse allograft model increases acute GVHD whereas the natural FFAR4 ligands and the synthetic FFAR4 agonists decrease it. Donor-T-cell-expressing *Ffar4* and recipient-expressing *Ffar4* are needed for FFAR4 agonism-mediated anti-acute GVHD effects. CpdA suppresses donor-T-cell mediated allo-reactivity by activating the β-Arrestin2/AhR/IL-22 pathway. CpdA recruits β-Arrestin2 to FFAR4 which facilitates nuclear translocation of AhR and upregulation of IL-22.

AhR belongs to the Pern-Arnt-Sim superfamily[24]. The role of AhR in GVHD was reported by two studies. Rohlman and co-authors found activation of AhR with its ligand prevented murine acute GVHD[25]. However, others showed *Ahr* knockout T-cells induced less severe acute GVHD in mice[26]. This discrepancy might attribute to the selectivity of strategies. In our study, T-cell conditioned knockout of *Ahr* blocked the CpdA-mediated anti-acute GVHD effect. AhR is a dominant regulator of IL-22 expression. We showed IL-22 expression was upregulated by FFAR4 agonism and was important for CpdA-mediated anti-acute GVHD effect. CpdA increased nuclear translocation of AhR. The expression of downstream gene *Cyp1a1* validated the activation of AhR. The clinical trial using recombinant IL-22 to treat GVHD recently reported that IL-22 treatment improved GVHD-associated dysbiosis and decreased gastrointestinal GVHD[27].

Tryptophan metabolites, the endogenous AhR ligands, contributed to homeostasis of intestinal epithelial barrier[28]. Others showed gut tryptophan metabolites activated AhR and protected intestinal epithelia through the IL-10 signaling[29]. We found allo-transplanted mice showed higher concentrations of tryptophan metabolites including 5-hydroxytryptophan, kynurenine and tryptophan comparing with untreated normal mice, however, CpdA did not alter levels of these tryptophan metabolites of allotransplanted mice (Fig. 4A). FFAR4 functions through the downstream GRK/β-Arrestin pathway and G-protein pathways[3]. We showed knockout of *Ffar4* decreased expression levels of genes such as GRK, PKC and PKA. Inhibitors of PKC and PKA did not block CpdA-induced expression of IL-22. In contrast, knockdown of β-Arrestin2 abolished this effect. Our pull-down assays indicated CpdA increased binding of AhR and ARNT. CpdA-treatment recruited β-Arrestin2 to FFAR4 on the cell membrane which was associated with increased nuclear translocation of AhR and increased binding of AhR and ARNT. HSP90 is a molecular chaperone of AhR. We confirmed the binding of HSP90 and AhR and the binding of β-Arrestin2 and HSP90 in the cytoplasm, and both were decreased by CpdA, which indicated β-Arrestin2 was released from the AhR complex after CpdA treatment. β-Arrestin2 in AhR complex might negatively regulate

Dynabeads. Supernatants of cell culture were used for measuring concentrations of cytokines (cytometric beads array for IL-6, TNFα and IFNγ, ELISA for IL-22) ($n = 4$). (F, G) CD3/CD28 Dynabeads-stimulated T-cells were treated by CpdA for 24 h. (F) Whole cell proteins were detected by Western blotting with indicated antibodies ($n = 3$). ImageJ was used to analyze band intensity. (G) RNA-seq analysis of T-cells treated by 10 μmol/L CpdA for 24 h. Figure shows the average of three independent values. Data are mean ± SD, compared using one-way ANOVA test or Student's *t* test. *$P < 0.05$; **$P < 0.01$; n.s., not significant.

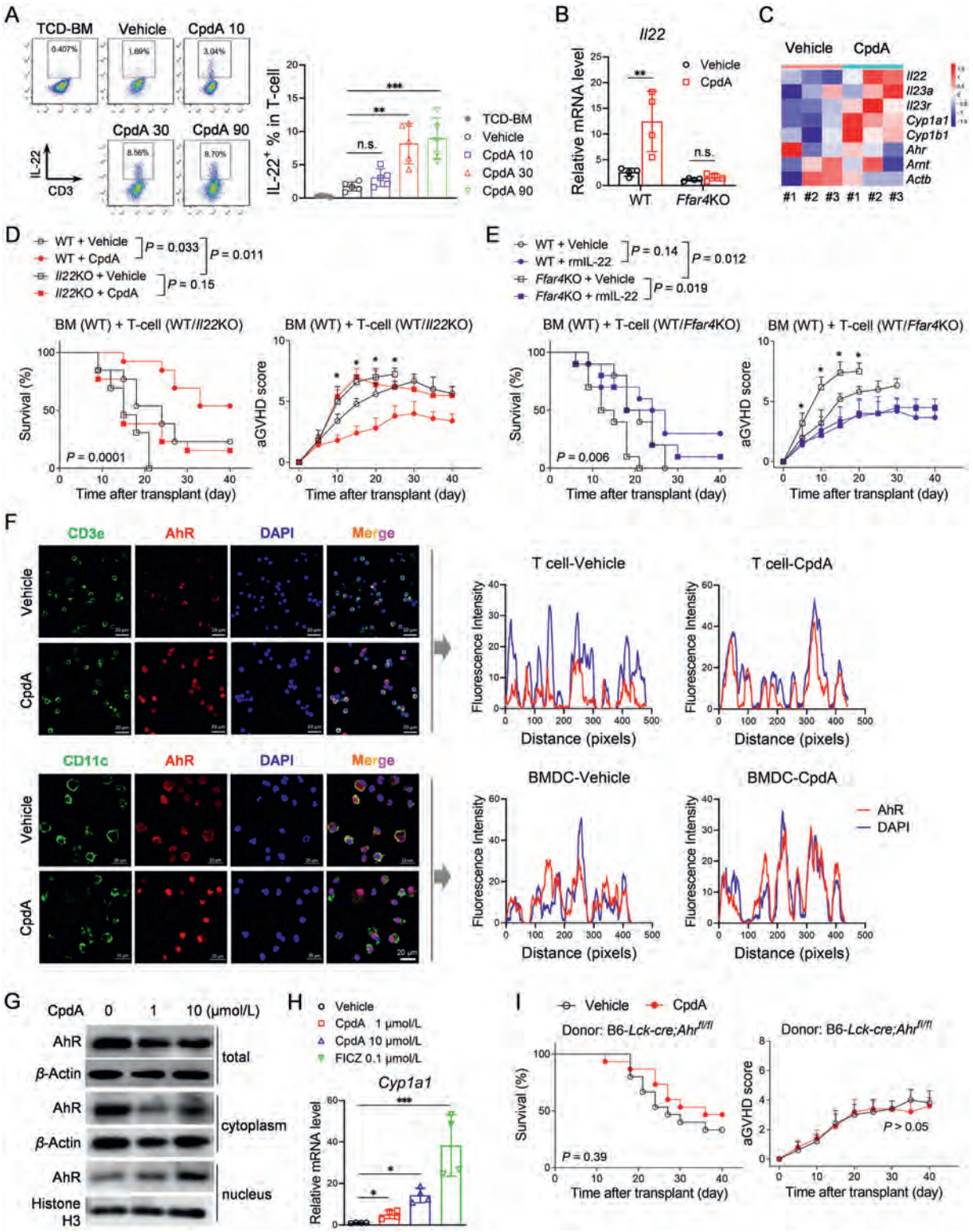

Figure 3 CpdA activated AhR/IL-22 in T-cells. (A) On Day 21, flow cytometry was used to analyze IL-22-positive spleen T-cells of recipient mice described in Fig. 1A ($n = 5$). (B) T-cells from WT or *Ffar4*KO B6 mice were stimulated by CD3/CD28 Dynabeads for 24 h in the presence of vehicle or 10 μmol/L CpdA. *Il-22* mRNA levels were measured by qPCR as described in Fig. 2E. (C) RNA-seq analysis of WT T-cells as described Fig. 2. All three replicates are shown. (D) In the B6 → BALB/c model, recipient mice were transplanted with WT or *Il22*KO T-cells. CpdA (30 mg/kg) injection was performed as described above. Survival and aGVHD score ($n = 13$ in each group). (E) In the B6 → BALB/c model, recipient mice were transplanted with WT or *Ffar4*KO T-cells. Recipient mice were injected with 10 μg/kg recombinant murine IL-22 twice weekly for 3 weeks. Survival and aGVHD score ($n = 10$ in each group). (F) CD3/CD28 Dynabeads-stimulated T-cells and LPS-primed BMDCs were treated by 10 μmol/L CpdA for 24 h. Cells were detected by immunofluorescence. ImageJ was used to analyze colocalization

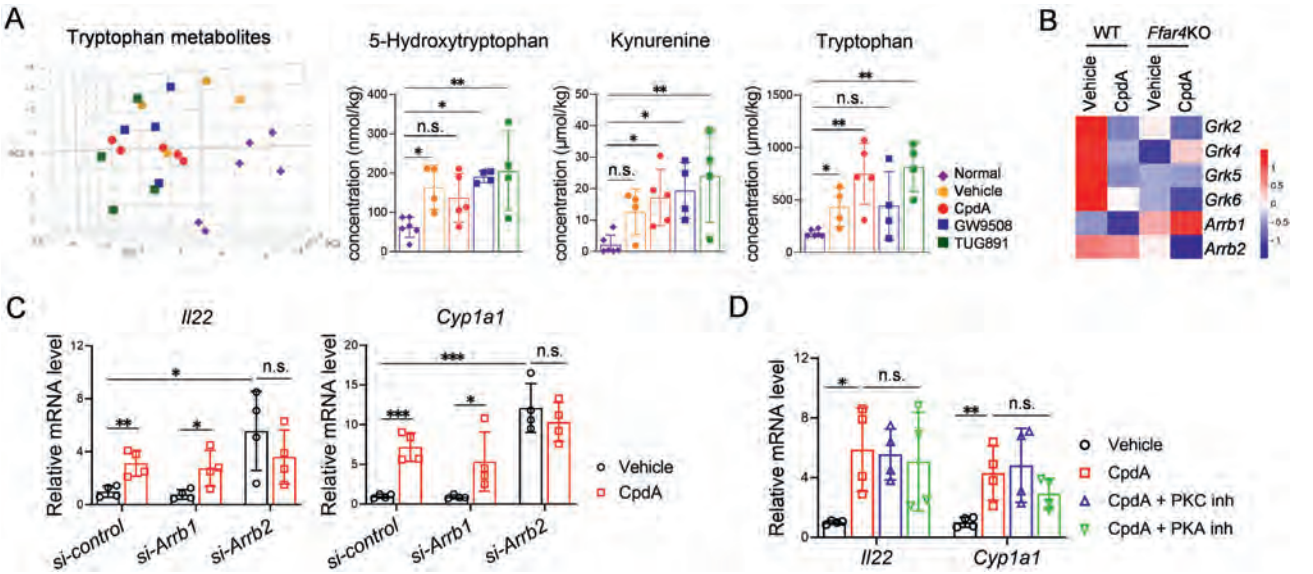

Figure 4 β-Arrestin2 was involved in activation of AhR/IL-22 pathway. (A) UHPLC−MS/MS analysis for tryptophan metabolites of fecal samples collected on Day 21 from recipient mice in the B6 → BALB/c model. Normal indicates mice not receiving an allotransplant ($n = 6$). Other mice all received an allotransplant and treated by vehicle ($n = 4$), CpdA ($n = 5$), GW9508 ($n = 4$) or TUG891 ($n = 4$). Concentrations of 5-hydroxytryptophan, kynurenine and tryptophan are shown. (B) RNA-seq analysis was described in Fig. 2. Figure shows the average of three independent values. (C) T-cells were transfected with 300 nmol/L siRNAs followed by stimulation with CD3/CD28 Dynabeads (48 h) and treatment with 10 μmol/L CpdA (24 h). mRNA levels were measured by qPCR ($n = 4$). (D) CD3/CD28 Dynabeads-stimulated T-cells were treated by 10 μmol/L CpdA for 24 h with/without a PKC inhibitor (1 μmol/L) and a PKA inhibitor (0.1 μmol/L). mRNA levels were measured by qPCR ($n = 4$). Data are mean ± SD, compared using one-way ANOVA test or Student's t test. $^*P < 0.05$; $^{**}P < 0.01$; $^{***}P < 0.001$; n.s., not significant.

nuclear translocation of AhR. Given the increased levels of tryptophan metabolites in allotransplanted mice, the recruitment of β-Arrestin2 by CpdA could facilitate nuclear translocation of AhR induced by these endogenous ligands. This is supported by the results that the nuclear translocation of AhR induced by FICZ was further enhanced by CpdA (Fig. 5E), and that knockdown of β-Arrestin2 increased nuclear translocation of AhR and expressions of *Il22* and *Cyp1a1* in T-cells (Figs. 5G, H and 4C). We found the AhR-HSP90 interaction was detectable in the nucleus (Fig. 5D), suggesting HSP90 shuttled to the nucleus together with AhR. This result is consistent with others' reports[30,31]. It remains unclear on the interactions of HSP90 and the AhR/ARNT complex in the nucleus, and the hypothesis is that a conformational change of AhR/ARNT complex causes dissociation of HSP90[24]. One study showed HSP90 was progressively released from AhR/ARNT complex[32], which is consistent with our result that HSP90 was absent in the immunoprecipitated proteins of ARNT antibody (Fig. 5D). Except for the major binding partner ARNT, AhR can bind with other proteins such as STAT members and RORγt[24]. On the other hand, the binding of AhR and ARNT could be inhibited by AHR repressor which might leave some AhR proteins at unbound status[33]. These points help to explain why we could detect the intra-nuclear binding of HSP90 and AhR but not of HSP90 and ARNT. The AhR complex showed dynamic changes in the nucleus[30], and more studies are needed to interpret this complicated process. Nonetheless, our results documented that CpdA increased nuclear translocation of AhR.

β-Arrestin can serve as an adaptor for other proteins[34,35]. GRK proteins are important in recruiting β-Arrestins to GPCR[36]. We found CpdA treatment or *Ffar4*KO decreased expression of GRK2, GRK4, GRK5 and GRK6, but not the other GRK proteins such as GRK1, GRK3 and GRK7. Expression level might not directly reflect the function of GRK, because recruitment and translocation are required for action of these GRK proteins[36], and intracellular trafficking of GPCR after agonism might have an impact on levels of these GRK proteins[37]. Moreover, expression of GRKs could be inhibited by pro-inflammatory factors[38], which were enhanced by *Ffar4*KO in our study. The specific GRK subtype involved in CpdA's effect is still to be defined.

CpdA decreased the pro-inflammatory profiles of T-cells in alloreactions such as MLR and IFNγ production, and these effects depended on *Ffar4*-exppression in T-cells. CpdA inhibited IFNγ production in co-cultured *Ffar4*KO T-cells and allogeneic BMDCs, but not in *Ffar4*KO T-cells cultured alone (Fig. 2E). The possible reason was CpdA decreased activation of BMDCs through FFAR4 because FFAR4 is also expressed on BMDCs (Fig. S3), and the

of AhR (red signal) and DAPI (blue signal). Figure shows one representative photo of three independent experiments. (G, H) CD3/CD28 Dynabeads-stimulated T-cells were treated by CpdA for 24 h. (G) Western blot analysis of AhR. Figure shows one representative band of three independent experiments. (H) *Cyp1a1* mRNA level was measured by qPCR ($n = 4$). The AhR agonist FICZ was used as a positive control. (I) In the B6 → BALB/c model, recipient mice were transplanted with *Lck-cre;Ahr*$^{fl/fl}$ T-cells. CpdA (30 mg/kg) injection was performed as described above. Survival and aGVHD score ($n = 15$ in each group). Survival was compared using log-rank test. Data were from three independent experiments. Data are mean ± SD, compared using one-way ANOVA test. $^*P < 0.05$; $^{**}P < 0.01$; $^{***}P < 0.001$; n.s., not significant.

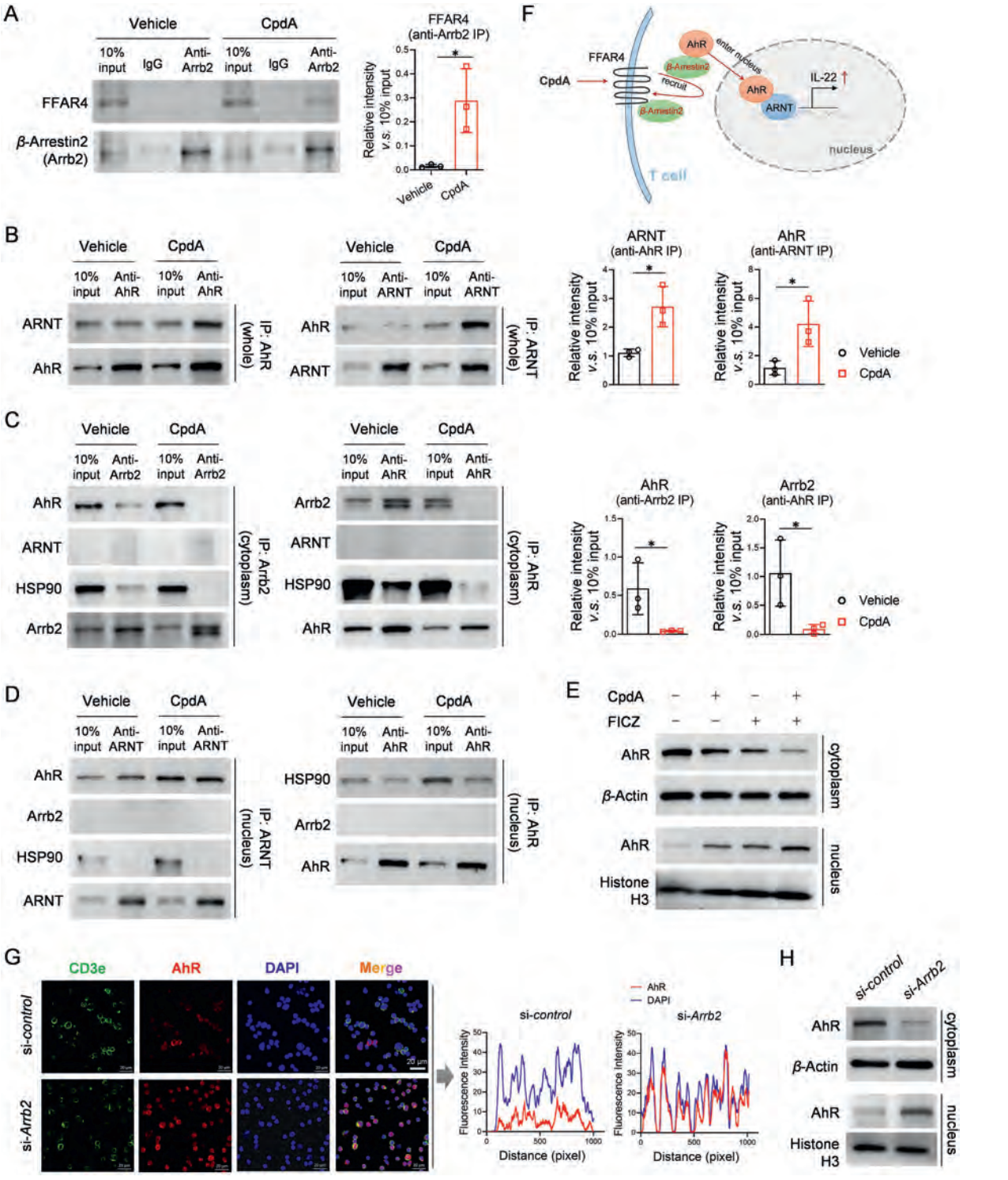

Figure 5 CpdA increased nuclear translocation of AhR. Immunoprecipitation was performed with whole cell proteins (A, B), cytoplastic proteins (C) or nuclear proteins (D) extracted from Jurkat cells. Anti-β-Arrestin2 (Arrb2), anti-AhR and anti-ARNT were used for pull-down assay. Western blot was used to detect proteins in precipitate. (E) Jurkat cells were treated by CpdA (10 μmol/L) or/and FICZ (0.1 μmol/L) for 24 h. Western blot was used to detect AhR in cytoplastic and nuclear proteins. (F) Proposed actions of CpdA in T-cell. (G, H) T-cells were transfected with siRNAs and stimulated by CD3/CD28 Dynabeads. (G) Cells were detected by immunofluorescence and analyzed as described in Fig. 3F. (H) Western blot was used to detect AhR in cytoplastic and nuclear proteins. Figures show representative result from three (A–C, G) or two (D, E, H) independent experiments. Data are mean ± SD, compared using Student's *t* test. $^*P < 0.05$.

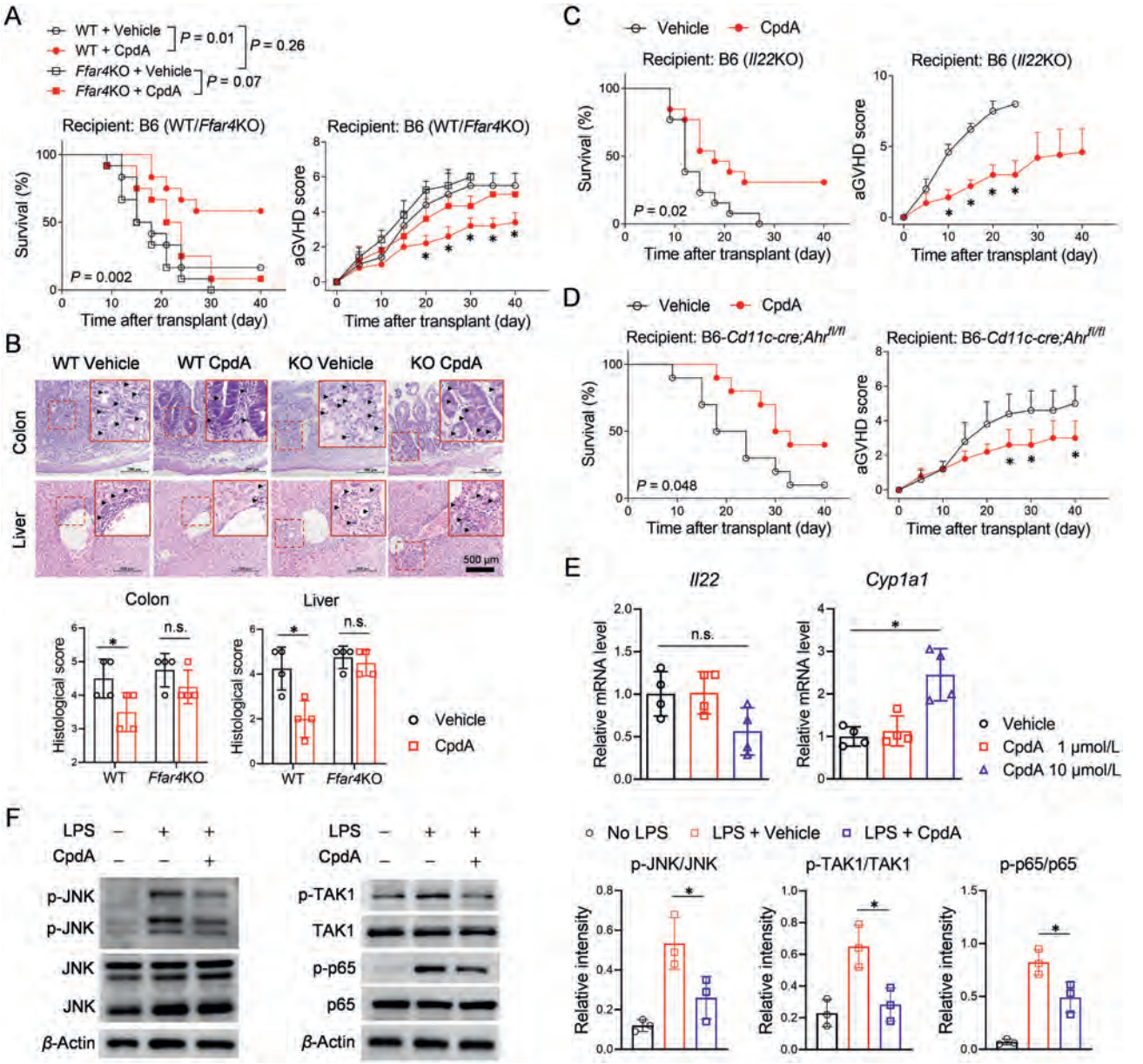

Figure 6 Recipient-expressing FFAR4 contributed to FFAR4 agonism-mediated anti-aGVHD effect. (A, B) In the BALB/c → B6 model, WT and *Ffar4*KO B6 mice were used as recipients. CpdA (30 mg/kg) injection was performed as described above. (A) Survival and aGVHD score ($n = 12$ in each group). (B) H&E staining and histological score ($n = 4$). (C, D) In the BALB/c → B6 model, *Il22*KO (C) and *CD11c-cre;Ahr*$^{fl/fl}$ (D) B6 mice were used as recipients. CpdA (30 mg/kg) injection was performed as described above. Survival and aGVHD score (*Il22*KO, $n = 13$; *CD11c-cre;Ahr*$^{fl/fl}$, $n = 10$). (E) LPS-primed BMDCs were treated by 10 μmol/L CpdA for 24 h mRNA levels were measured by qPCR ($n = 4$). (F) BMDCs treated or not treated by LPS and CpdA. Western blot analysis of proteins as indicated ($n = 3$). Survival was compared using log-rank test. Data were from three independent experiments. Data are mean ± SD, compared using one-way ANOVA test or Student's *t* test. *$P < 0.05$; n.s., not significant.

inhibition on BMDCs might contribute to the decreased IFNγ production in co-cultures. Furthermore, CpdA decreased phosphorylation of STAT1 and STAT3. STAT1 transduces signals from interferons, whereas STAT3 is responsible for IL-6 and other gp130 cytokines[39]. This is consistent with the results that CpdA decreased production of IL-6 and IFNγ, and knockout of *Ffar4* increased production of these two cytokines. Some other studies reported the correlation between FFAR4 and STAT3. The FFAR4 agonist TUG891 decreased STAT3 phosphorylation in podocytes and ameliorated renal inflammation[17]. Omega-3 PUFAs downregulated STAT3 phosphorylation in dendritic cells and alleviated experimental autoimmune encephalomyelitis[40].

Recipient APCs are needed to activate donor T-cells in acute GVHD[1]. We found the FFAR4 agonist inhibited activation of APCs. Recipient derived *Ffar4* was important for CpdA-mediated anti-acute GVHD effect. However, the anti-acute GVHD effect of recipient FFAR4 did not depend on recipient-derived AhR or IL-22, because CpdA could alleviate acute GVHD in *Ahr*KO recipients and *Il22*KO recipients. This is supported by the result that CpdA did not increase *Il22* expression in recipient dendritic cells (Fig. 6E

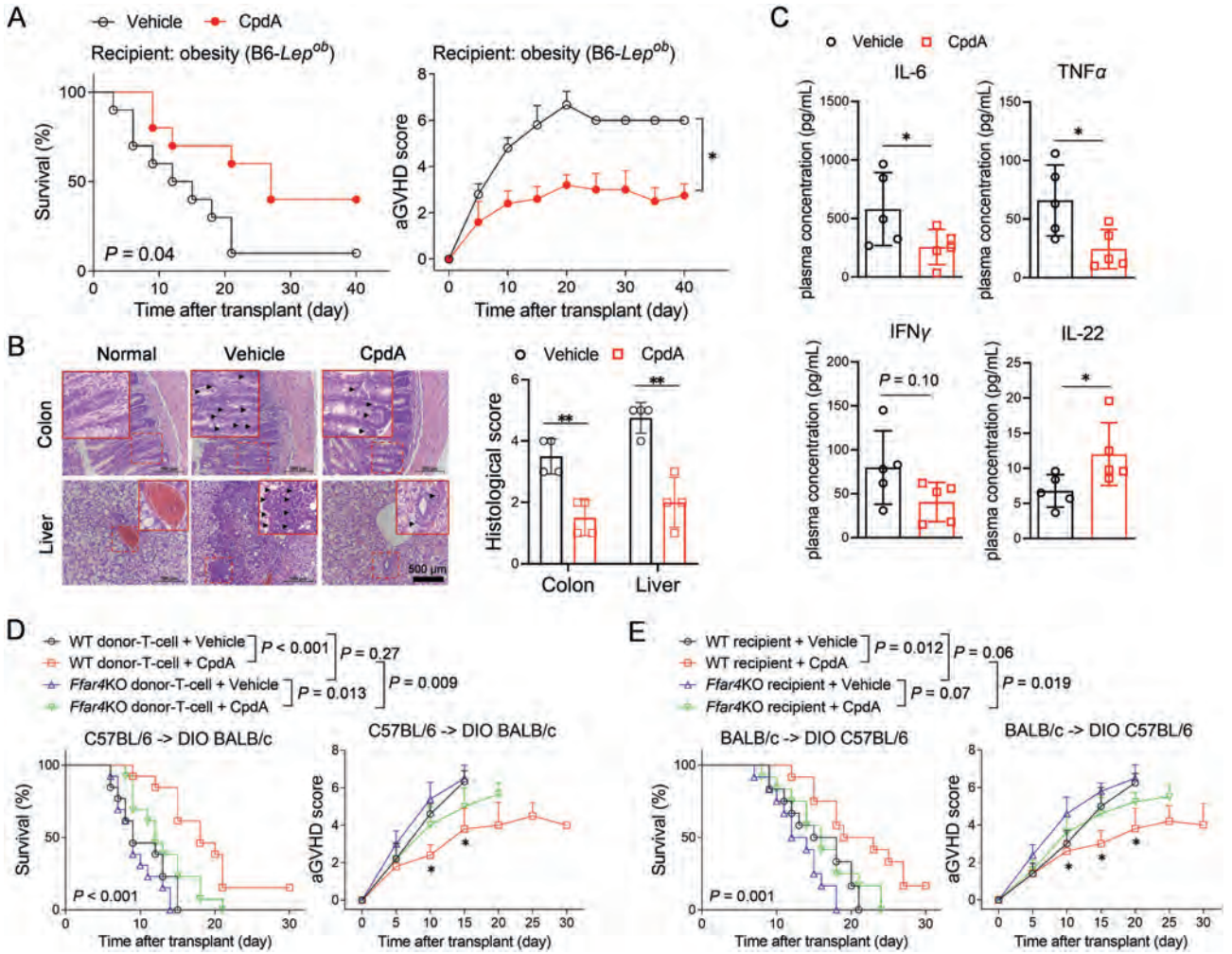

Figure 7 FFAR4 agonism alleviated aGVHD in obese mice. In the BALB/c → B6 model, *Lep*^{ob} obesity B6 mice were used as recipients. CpdA (30 mg/kg) injection was performed as described. (A) Survival and aGVHD score ($n = 10$ in each group). (B) H&E staining and histological score ($n = 4$). Normal group indicated the obesity mice were not treated by irradiation or transplant. (C) Plasma samples were used for measuring concentrations of cytokines as described ($n = 5$). (D) In the B6 → BALB/c model, diet-induced obesity (DIO) BALB/c mice were recipients. Recipient mice received WT or *Ffar4*KO T-cells ($n = 13$ in each group). (E) In the BALB/c → B6 model, DIO mice derived from WT or *Ffar4*KO B6 mice were used as recipients ($n = 12$ in each group). CpdA (30 mg/kg) injection was performed as described. Survival and aGVHD score were recorded. Survival was compared using log-rank test. Data were from two independent experiments. Data are mean ± SD, compared using Student's *t* test. $^*P < 0.05$; $^{**}P < 0.01$; n.s., not significant.

and Fig. S5). T-cells and innate lymphoid cells are dominant producers of IL-22[23]. We found CpdA increased activation of AhR in BMDCs (Figs. 3F and 6E), however, the AhR agonist FICZ did not increase *Il22* expression in BMDCs (data not shown) indicating IL-22 was not a target of CpdA in APCs and AhR-activation in APCs might not upregulate *Il22* expression. Others reported that FFAR4 agonism suppressed activation of macrophages through inhibition of JNK and TAK1 activation[8,9]. We also found CpdA decreased phosphorylation of JNK, TAK1 and p65 in BMDCs, and decreased production of IL-6 and TNFα in BMDCs. IL-6 and TNFα are well proved mediators of acute GVHD[41].

CpdA also decreases acute GVHD in obese mice. The comparisons between survivals of regular recipients and DIO recipients indicated CpdA might provide a more significant protective function in DIO recipients. In regular recipients, CpdA-mediated anti-acute GVHD effect was abolished by *Ffar4*KO in donor T-cells. In contrast, CpdA could still protect DIO recipients receiving *Ffar4*KO T-cells, suggesting CpdA might exert other protective functions in addition to inhibition of T-cells. CpdA was reported to ameliorate metabolic disorders in obese mice[8,9]. The *Lep*^{ob} mice used in our study have obesity-related diabetes. CpdA is also a SHIP2 inhibitor which could protect these mice through inhibition of SHIP2, because SHIP2 was shown to increase insulin resistance in diabetic mice[42]. Although SHIP2 is primarily expressed in nonhematopoietic tissues including heart, skeletal muscle and fat, others also found the expression of SHIP2 in human T-cells[43,44]. It remains unclear whether CpdA functions through SHIP2 or whether FFAR4 cross-talks with SHIP2 in acute GVHD. Thus, targeting FFAR4 might be an option for controlling acute GVHD in obese recipients.

Our study has limitations. We focused on the β-Arrestin2 pathway in T-cells. The other G-protein pathways might also mediate the effect of FFAR4 agonism. We found *Ffar4*KO decreased expression of G-protein pathways-related genes in

T-cells such as G-protein subunits and PI3K subunits (Fig. S7). Others had reported agonism of FFAR4 activated the G-protein pathways such as Gq protein and PI3K[45,46]. These pathways also regulate T-cell functions[47]. Although the synthetic FFAR4 agonists we used have high selectivity and efficacy[8,9,48], there might be possible off-target effects of these agonists. CpdA induced changes in gene expression independent of FFAR4, such as IL-4 and IL-7 in T-cells (Fig. S7).

5. Conclusions

In summary, our study shows the immune regulatory effect of FFAR4 in allogeneic reactions with possible implications for using FFAR4 ligands or agonists to control acute GVHD in humans especially those who with obesity.

Acknowledgments

This study was supported by National Natural Science Foundation of China (82170214, 81970159 and 82370218 to Bin Pan, 81930005 and 82341203 to Kailin Xu), the Jiangsu Provincial Key Research and Development Program (BE2021631 to Bin Pan, China), and the Natural Science Research of Jiangsu Higher Education Institutions of China (20KJA320002 to Bin Pan). Prof. Robert Peter Gale (Imperial College of Science, Technology and Medicine) kindly revised the typescript.

Author contributions

Maxwell Duah: Writing − original draft, Project administration, Methodology, Investigation. Fei Zheng: Project administration, Methodology, Investigation. Jingyi Shen: Project administration, Methodology, Investigation. Yan Xu: Project administration, Methodology, Investigation. Shuo Cao: Validation, Project administration. Zhiling Yan: Validation, Project administration. Qiu Lan: Validation, Project administration. Ying Wang: Validation, Project administration. Kailin Xu: Writing − review & editing, Supervision, Resources, Funding acquisition. Bin Pan: Writing − review & editing, Funding acquisition, Formal analysis, Data curation, Conceptualization.

Conflicts of interest

The authors declare no conflicts of interest.

Appendix A. Supporting information

Supporting information to this article can be found online at https://doi.org/10.1016/j.apsb.2024.12.011.

References

1. Zeiser R, Blazar BR. Acute graft-*versus*-host disease−biologic process, prevention, and therapy. *N Engl J Med* 2017;**377**:2167−79.
2. Penack O, Marchetti M, Ruutu T, Aljurf M, Bacigalupo A, Bonifazi F, et al. Prophylaxis and management of graft *versus* host disease after stem-cell transplantation for haematological malignancies: updated consensus recommendations of the European Society for Blood and Marrow Transplantation. *Lancet Haematol* 2020;**7**:157−67.
3. Tan JK, McKenzie C, Marino E, Macia L, Mackay CR. Metabolite-sensing g protein-coupled receptors-facilitators of diet-related immune regulation. *Annu Rev Immunol* 2017;**35**:371−402.
4. Duah M, Zhang K, Liang Y, Ayarick VA, Xu K, Pan B. Immune regulation of poly unsaturated fatty acids and free fatty acid receptor 4. *J Nutr Biochem* 2023;**112**:109222.
5. Oh H, Loberiza Jr FR, Zhang MJ, Ringden O, Akiyama H, Asai T, et al. Comparison of graft-*versus*-host-disease and survival after HLA-identical sibling bone marrow transplantation in ethnic populations. *Blood* 2005;**105**:1408−16.
6. Aljurf MD, Zaidi SZ, El Solh H, Hussain F, Ghavamzadeh A, Mahmoud HK, et al. Special issues related to hematopoietic SCT in the Eastern Mediterranean region and the first regional activity report. *Bone Marrow Transpl* 2009;**43**:1−12.
7. Takatsuka H, Takemoto Y, Iwata N, Suehiro A, Hamano T, Okamoto T, et al. Oral eicosapentaenoic acid for complications of bone marrow transplantation. *Bone Marrow Transpl* 2001;**28**:769−74.
8. Oh DY, Walenta E, Akiyama TE, Lagakos WS, Lackey D, Pessentheiner AR, et al. A Gpr120-selective agonist improves insulin resistance and chronic inflammation in obese mice. *Nat Med* 2014;**20**: 942−7.
9. Oh DY, Talukdar S, Bae EJ, Imamura T, Morinaga H, Fan W, et al. GPR120 is an omega-3 fatty acid receptor mediating potent anti-inflammatory and insulin-sensitizing effects. *Cell* 2010;**142**:687−98.
10. Weiss BM, Vogl DT, Berger NA, Stadtmauer EA, Lazarus HM. Trimming the fat: obesity and hematopoietic cell transplantation. *Bone Marrow Transpl* 2013;**48**:1152−60.
11. Wieduwilt MJ, Stock W, Advani A, Luger S, Larson RA, Tallman M, et al. Superior survival with pediatric-style chemotherapy compared to myeloablative allogeneic hematopoietic cell transplantation in older adolescents and young adults with Ph-negative acute lymphoblastic leukemia in first complete remission: analysis from CALGB 10403 and the CIBMTR. *Leukemia* 2021;**35**:2076−85.
12. Khuat LT, Le CT, Pai CS, Shields Cutler RR, Holtan SG, Rashidi A, et al. Obesity induces gut microbiota alterations and augments acute graft-versus-host disease after allogeneic stem cell transplantation. *Sci Transl Med* 2020;**12**:eaay7713.
13. Rohm TV, Meier DT, Olefsky JM, Donath MY. Inflammation in obesity, diabetes, and related disorders. *Immunity* 2022;**55**:31−55.
14. Sorror ML, Maris MB, Storb R, Baron F, Sandmaier BM, Maloney DG, et al. Hematopoietic cell transplantation (HCT)-specific comorbidity index: a new tool for risk assessment before allogeneic HCT. *Blood* 2005;**106**:2912−9.
15. Gao J, Xu Y, Ma S, Liang Y, Liu C, Shen J, et al. Inhibition of IL-1 receptor-associated kinase 1 decreases murine acute graft-*versus*-host disease while preserving the graft-*versus*-lymphoma effect. *Transpl Cell Ther* 2022;**28**:134.e1. 10.
16. Konigs V, Pierre S, Schicht M, Welss J, Hahnefeld L, Rimola V, et al. GPR40 activation abolishes diabetes-induced painful neuropathy by suppressing VEGF-A expression. *Diabetes* 2022;**71**:774−87.
17. Wei TT, Yang LT, Guo F, Tao SB, Cheng L, Huang RS, et al. Activation of GPR120 in podocytes ameliorates kidney fibrosis and inflammation in diabetic nephropathy. *Acta Pharmacol Sin* 2021;**42**: 252−63.
18. Cooke KR, Kobzik L, Martin TR, Brewer J, Delmonte Jr J, Crawford JM, et al. An experimental model of idiopathic pneumonia syndrome after bone marrow transplantation: I. The roles of minor H antigens and endotoxin. *Blood* 1996;**88**:3230−9.
19. Kaplan DH, Anderson BE, McNiff JM, Jain D, Shlomchik MJ, Shlomchik WD. Target antigens determine graft-*versus*-host disease phenotype. *J Immunol* 2004;**173**:5467−75.
20. Kimura I, Ichimura A, Ohue Kitano R, Igarashi M. Free fatty acid receptors in health and disease. *Physiol Rev* 2020;**100**:171−210.
21. Pan B, Wang D, Li L, Shang L, Xia F, Zhang F, et al. IL-22 accelerates thymus regeneration *via* Stat3/Mcl-1 and decreases chronic graft-*versus*-host disease in mice after allotransplants. *Biol Blood Marrow Transpl* 2019;**25**:1911−9.
22. Hanash AM, Dudakov JA, Hua G, O'Connor MH, Young LF, Singer NV, et al. Interleukin-22 protects intestinal stem cells from immune-mediated tissue damage and regulates sensitivity to graft *versus* host disease. *Immunity* 2012;**37**:339−50.

23. Dudakov JA, Hanash AM, van den Brink MR. Interleukin-22: immunobiology and pathology. *Annu Rev Immunol* 2015;**33**:747−85.
24. Gutierrez Vazquez C, Quintana FJ. Regulation of the immune response by the aryl hydrocarbon receptor. *Immunity* 2018;**48**:19−33.
25. Rohlman D, Punj S, Pennington J, Bradford S, Kerkvliet NI. Suppression of acute graft-*versus*-host response by TCDD is independent of the CTLA-4−IFN-γ−IDO pathway. *Toxicol Sci* 2013;**135**:81−90.
26. Dant TA, Lin KL, Bruce DW, Montgomery SA, Kolupaev OV, Bommiasamy H, et al. T-cell expression of AhR inhibits the maintenance of pT_{reg} cells in the gastrointestinal tract in acute GVHD. *Blood* 2017;**130**:348−59.
27. Ponce DM, Alousi AM, Nakamura R, Slingerland J, Calafiore M, Sandhu KS, et al. A phase 2 study of interleukin-22 and systemic corticosteroids as initial treatment for acute GVHD of the lower GI tract. *Blood* 2023;**141**:1389−401.
28. Roager HM, Licht TR. Microbial tryptophan catabolites in health and disease. *Nat Commun* 2018;**9**:3294.
29. Lanis JM, Alexeev EE, Curtis VF, Kitzenberg DA, Kao DJ, Battista KD, et al. Tryptophan metabolite activation of the aryl hydrocarbon receptor regulates IL-10 receptor expression on intestinal epithelia. *Mucosal Immunol* 2017;**10**:1133−44.
30. Tsuji N, Fukuda K, Nagata Y, Okada H, Haga A, Hatakeyama S, et al. The activation mechanism of the aryl hydrocarbon receptor (AhR) by molecular chaperone HSP90. *FEBS Open Bio* 2014;**4**:796−803.
31. Kudo I, Hosaka M, Haga A, Tsuji N, Nagata Y, Okada H, et al. The regulation mechanisms of AhR by molecular chaperone complex. *J Biochem* 2018;**163**:223−32.
32. Soshilov AA, Motta S, Bonati L, Denison MS. Transitional States in ligand-dependent transformation of the aryl hydrocarbon receptor into its DNA-Binding form. *Int J Mol Sci* 2020;**21**:2474.
33. Rothhammer V, Quintana FJ. The aryl hydrocarbon receptor: an environmental sensor integrating immune responses in health and disease. *Nat Rev Immunol* 2019;**19**:184−97.
34. Smith JS, Rajagopal S. The β-arrestins: multifunctional regulators of G protein-coupled receptors. *J Biol Chem* 2016;**291**:8969−77.
35. Xie Q, Chu Y, Yuan W, Li Y, Li K, Wu X, et al. Activation of insulin-like growth factor-1 receptor (IGF-1R) promotes growth of colorectal cancer through triggering the MEX3A-mediated degradation of RIG-I. *Acta Pharm Sin B* 2023;**13**:2963−75.
36. Pfleger J, Gresham K, Koch WJ. G protein-coupled receptor kinases as therapeutic targets in the heart. *Nat Rev Cardiol* 2019;**16**:612−22.
37. Moore CA, Milano SK, Benovic JL. Regulation of receptor trafficking by GRKs and arrestins. *Annu Rev Physiol* 2007;**69**:451−82.
38. Ribas C, Penela P, Murga C, Salcedo A, Garcia Hoz C, Jurado Pueyo M, et al. The G protein-coupled receptor kinase (GRK) interactome: role of GRKs in GPCR regulation and signaling. *Biochim Biophys Acta* 2007;**1768**:913−22.
39. O'Shea JJ, Schwartz DM, Villarino AV, Gadina M, McInnes IB, Laurence A. The JAK−STAT pathway: impact on human disease and therapeutic intervention. *Annu Rev Med* 2015;**66**:311−28.
40. Feng C, Li L, Li Q, Switzer K, Liu M, Han S, et al. Docosahexaenoic acid ameliorates autoimmune inflammation by activating GPR120 signaling pathway in dendritic cells. *Int Immunopharmacol* 2021;**97**:107698.
41. Choi SW, Reddy P. Current and emerging strategies for the prevention of graft-*versus*-host disease. *Nat Rev Clin Oncol* 2014;**11**:536−47.
42. Ichihara Y, Fujimura R, Tsuneki H, Wada T, Okamoto K, Gouda H, et al. Rational design and synthesis of 4-substituted 2-pyridin-2-ylamides with inhibitory effects on SH2 domain-containing inositol 5′-phosphatase 2 (SHIP2). *Eur J Med Chem* 2013;**62**:649−60.
43. Hori H, Sasaoka T, Ishihara H, Wada T, Murakami S, Ishiki M, et al. Association of SH2-containing inositol phosphatase 2 with the insulin resistance of diabetic *db/db* mice. *Diabetes* 2002;**51**:2387−94.
44. Bruyns C, Pesesse X, Moreau C, Blero D, Erneux C. The two SH2-domain-containing inositol 5-phosphatases SHIP1 and SHIP2 are coexpressed in human T lymphocytes. *Biol Chem* 1999;**380**:969−74.
45. Yang L, Wang B, Guo F, Huang R, Liang Y, Li L, et al. FFAR4 improves the senescence of tubular epithelial cells by AMPK/SirT3 signaling in acute kidney injury. *Signal Transduct Target Ther* 2022;**7**:384.
46. Katsuma S, Hatae N, Yano T, Ruike Y, Kimura M, Hirasawa A, et al. Free fatty acids inhibit serum deprivation-induced apoptosis through GPR120 in a murine enteroendocrine cell line STC-1. *J Biol Chem* 2005;**280**:19507−15.
47. Smith-Garvin JE, Koretzky GA, Jordan MS. T cell activation. *Annu Rev Immunol* 2009;**27**:591−619.
48. Milligan G, Alvarez Curto E, Hudson BD, Prihandoko R, Tobin AB. FFA4/GPR120: pharmacology and therapeutic opportunities. *Trends Pharmacol Sci* 2017;**38**:809−21.